Nonlinear interactions in an organic polariton condensate

K. S. Daskalakis, S. A. Maier, R. Murray and S. Kéna-Cohen

SUPPLEMENTARY INFORMATION

1. Angle-resolved reflectivity spectra

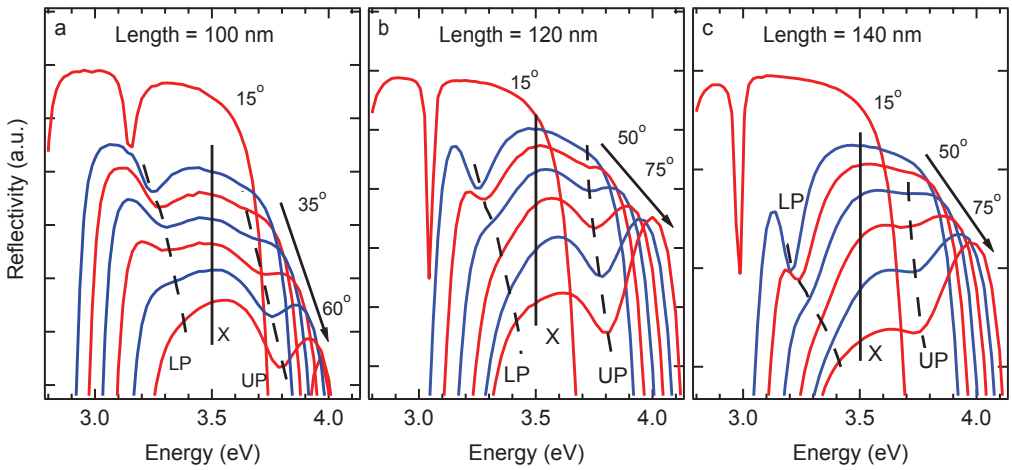


Fig. S1: Angle-resolved reflectivity spectra measured for (a) 100 (b) 120 and c) 140 nm thick cavities. On these spectra, both the upper and lower polariton branches can be readily identified (squares). These were used for the coupled harmonic oscillator (CHO) fit in the Methods section. Note the weaker upper branch dip due the large oscillator impedance mismatch and negative detuning. This dip is difficult to resolve on the contour plot from Fig. 1, but its identification from the spectra increases the reliability of the CHO fit parameters. The 100 nm cavity shown here did not exhibit lasing due to ineffective pumping of the LP at high energy.

We have also fabricated identical cavities with only 4 top DBR pairs. This slightly reduces the cavity Q, but greatly increases the upper branch dip visibility. These were used to identify the upper branch position for TE polarization. Indeed, the upper branch is

more difficult to resolve for TE polarization in high Q organic cavities, due the background absorption on the high energy side of the exciton resonance.[22]

2. LP dispersion relations

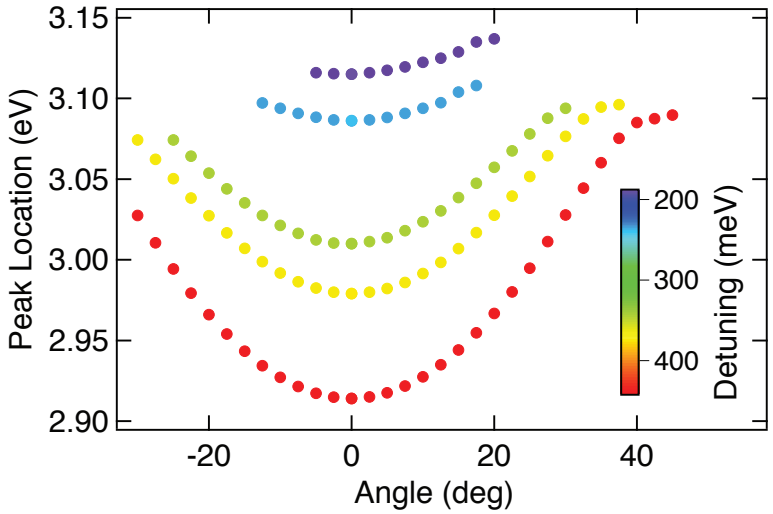


Fig. S2: LP dispersion relation of all of the fabricated microcavities. The Figure includes both τ_{LP} ~ 55 fs and τ_{LP} ~ 150 fs microcavities with identical mirror stacks, but increasing numbers of pairs. Note the flattening out of the LP dispersion away from the exciton resonance characteristic of polaritonic behaviour as the detuning is made more positive.

3. Comparison with metal cavities

A direct comparison can be drawn between the results obtained in Ref. [35] using metal mirrors and those shown in Table 1. Using the notation of Ref. [35], the dielectric constant of TDAF is taken as:

$$\varepsilon(\omega) = \varepsilon_B + \frac{A}{\omega_{ex}^2 - \omega^2} \approx \varepsilon_B + \frac{A/2\omega_{ex}}{\omega_{ex} - \omega}$$

where in the second step we make the rotating wave approximation. The dispersion relation (at normal incidence) is given by:

$$r_M(\omega)\exp\left(i\frac{\omega}{c}n(\omega)d\right)=\pm 1$$

where $n(\omega)\approx\sqrt{\varepsilon_B}+\frac{A/\left(4\omega_{ex}\sqrt{\varepsilon_B}\right)}{\omega_{ex}-\omega}\equiv n_B+n''(\omega)$ is the refractive index and $r_M(\omega)=\exp\left(i\frac{n(\omega)}{c}L_{DBR}(\omega-\omega_{ex})\right)$ is the phase change upon reflection from a Bragg mirror with penetration depth L_{DBR} and stopband centered at ω_{ex} (see Refs. [2,45]).

The bare cavity mode frequency can be found by setting $n(\omega) = n_B$ in the dispersion relation. We obtain:

$$\omega_c=\frac{m\pi c+n_B L_{DBR}\omega_{ex}}{n_B(L_{DBR}+d)}$$

The dispersion equation then reads:

$$(\omega-\omega_{ex})(\omega-\omega_c)n_B(d+L_{DBR})=\frac{A}{4\omega_{ex}n_B}\left[\omega d+(\omega-\omega_{ex})L_{DBR}\right]$$

By making the usual CHO approximation $\omega\approx\omega_{ex}$ we obtain:

$$(\omega-\omega_{ex})(\omega-\omega_c)=V^2$$

where:

$$V^2\equiv\frac{A}{4n_B^2}\left(\frac{d}{d+L_{DBR}}\right)$$

is as defined in the text. From this expression, we can identify the fit parameter $V_0\equiv\sqrt{A/4\varepsilon_B}$ defined in the text, which depends only on material parameters.

The Rabi splittings, Ω, extracted in Ref. [35] also depend only on A and ε_B, via the expression $\Omega = \sqrt{A/\varepsilon_B}$, derived in that work for metal mirrors.

The values of V_0 from Table 1 can thus be readily compared with the Rabi splittings, Ω, extracted in Ref. [35] using the correspondence $\Omega = 2V_0$ and indeed, the agreement is excellent.

3. Transverse electric angle-resolved photoluminescence

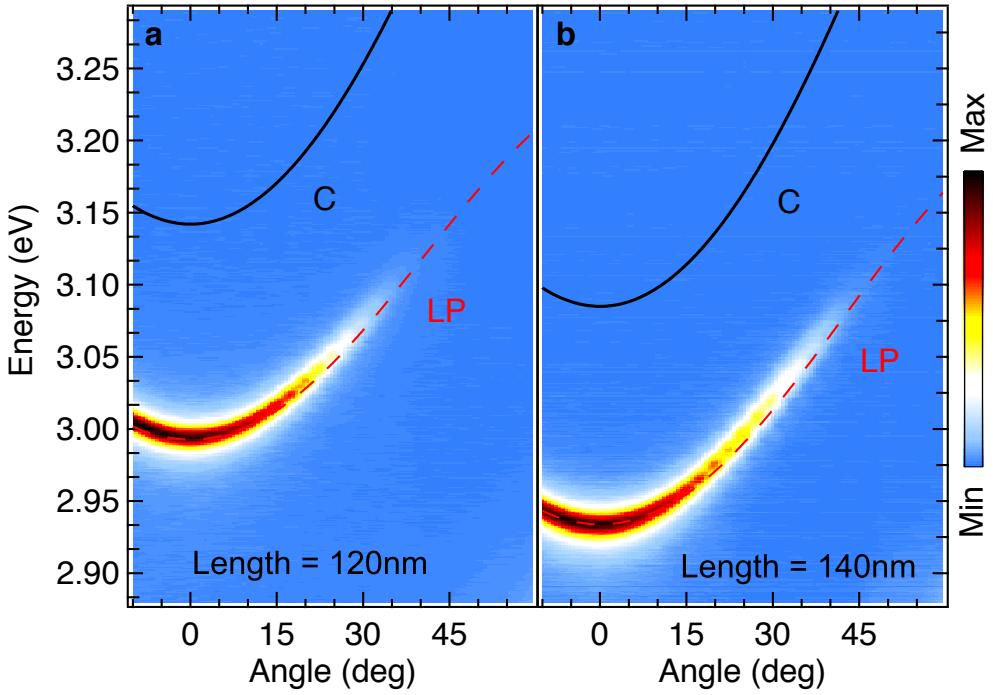


Fig. S3: Angle-resolved photoluminescence measured for the a) 120 nm and b) 140 nm thick microcavities below threshold. The dashed lines show the fit obtained from the CHO model. The measured dispersion is in good agreement with that obtained from reflectivity given the different spot locations for both experiments.

4. Additional measurements for increasing pump fluence

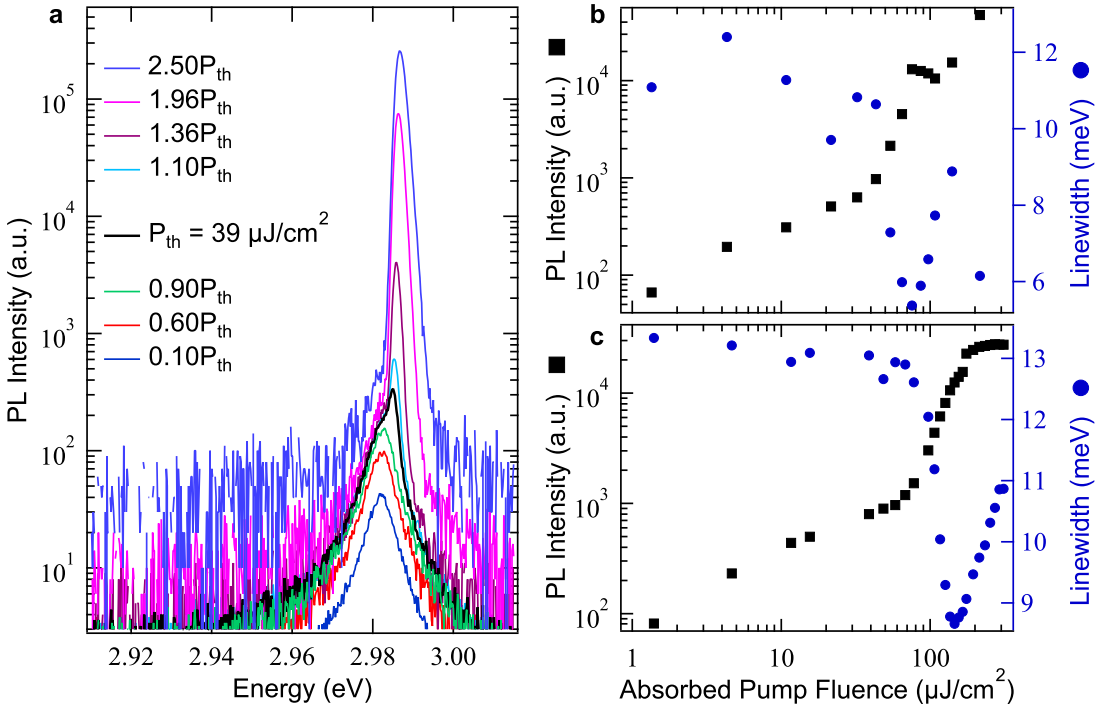


Fig. S4: a) Measured spectra for a 120 nm thick TDAF microcavity sandwiched between 2 DBRs composed of 9 mirror pairs. The extracted LP lifetime, based on the LP linewidth is τ_{LP} ~ 150 fs. Note the reduced threshold by approximately a factor of 2 over that shown in the text, concomitant with the longer LP lifetime and the reduced blueshift. b) Pump fluence dependence of the peak intensity and linewidth for the 6 pair 120 nm thick cavity when a smaller 44 x 61 μm pump spot is used. The observed behavior is nearly identical to the larger spot from the text. The measured threshold pump fluence is slightly lower (P_{th} ~ 42 μJ/cm^2) and the double kink observed around 100 μJ/cm^2 is ascribed to slight photodamage, as opposed to a second transition to photon lasing as is sometimes seen in inorganic semiconductor microcavities. Note that the energy needed to reach threshold for this spot size is only 880 pJ. c) Pump fluence dependence of the peak intensity and linewidth for the 140 nm thick 6 pair cavity described in the text.